3

Fluorescence-guided Resection of Experimental Malignant Glioma Using Cetuximab-IRDye800CW

J. M. Warram,[1] **E. de Boer**,[1,2] M. L. Korb,[1] Y. E. Hartman,[1] J. Kovar,[3] J. M. Markert,[2] G. Y. Gillespie[2] and E. L. Rosenthal[1]

1. Department of Surgery, University of Alabama at Birmingham, USA.
2. Department of Surgery, University Medical Centre Groningen, University of Groningen, The Netherlands.
3. LI-COR Biosciences, Lincoln, Nebraska, USA.

Published in **British Journal of Neurosurgery, December 2015,** 29(6):850-8.
DOI: 10.3109/02688697.2015.1056090

ABSTRACT

The standard treatment for Glioblastoma Multiforme (GBM) remains maximal safe surgical resection. Here, we evaluated the ability of a systemically administered antibody-dye probe conjugate (cetuximab-IRDye 800CW) to provide sufficient fluorescent contrast for surgical resection of disease in both subcutaneous and orthotopic animal models of GBM. Multiple luciferase positive GBM cell lines (D-54MG, U-87MG, U-251MG; n=5) were implanted in mouse flank and tumours fluorescently imaged daily using a closed-field NIR system after cetuximab-IRDye 800CW systemic administration. Orthotopic models were also generated (n=5) and tumour resection was performed under white-light and fluorescence guidance using an FDA-approved wide-field NIR imaging system. Residual tumour was monitored using luciferase imaging. Immunohistochemistry was performed to characterize tumour fluorescence, epidermal growth factor receptor (EGFR) expression, and vessel density. Daily imaging of tumours revealed an average tumour-to-background (TBR) of 4.5 for U-87MG, 4.1 for D-54MG, and 3.7 for U-251MG. Fluorescence intensity within the tumours peaked on day-1 post cetuximab-IRDye 800CW administration, however the TBR increased over time in two of the three cell lines. For the orthotopic model, TBR on surgery day ranged from 19 to 23 during wide-field, intraoperative imaging. Surgical resection under white-light on day 3 post cetuximab-IRDye 800CW resulted in an average 41% reduction in luciferase signal while fluorescence-guided resection using wide-field NIR imaging resulted in a significantly ($P=0.001$) greater reduction in luciferase signal (87%). Reduction of luciferase signal was found to correlate ($R^2=0.99$) with reduction in fluorescence intensity. Fluorescence intensity was found to correlate ($P<0.05$) with EGFR expression in D-54MG and U-251MG tumour types but not U-87MG. However, tumour fluorescence was found to correlate with vessel density for the U-87MG tumours. Here we show systemic administration of cetuximab-IRDye 800CW in combination with wide-field NIR imaging provided robust and specific fluorescence contrast for successful localization of disease in subcutaneous and orthotopic animal models of GBM.

INTRODUCTION

Maximal safe surgical resection remains the primary standard of care for the treatment of Glioblastoma Multiforme (GBM). Retrospective studies have provided substantial evidence that extent of resection is a predictor of survival with anywhere between a 70% and 98% extent of resection required to positively impact survival and a maximum post-resection residual volume of 5cm^3 required to reach a threshold that increases median survival.[1-3] In one clinical study, researchers found that total resection (>95%) led to a median survival of 19 months compared to a median survival of 15.9 months for patients that received partial resection.[4] GBM is characteristically infiltrative with poorly defined margins. Neoplastic cells often migrate along axonal fibers and perivascular spaces deep within the tissue and beyond the preoperatively mapped disease site,[5] such that discernment of the tumour border zone is challenging even at the histopathological level.[6,7] While ongoing refinements in surgical techniques are encouraging, a major methodological limitation has remained the inability of the surgeon to visualize cancer from normal tissue during microscopic resection. Compounding this limitation is the inability of the surgeon to mechanically palpate potential disease areas during microsurgical procedures. In some cases, the lack of sufficient contrast to delineate infiltrative tumour borders in eloquent areas has discouraged surgical treatment altogether.[8,9] These limitations illustrate the need for novel intraoperative techniques to improve tumour residual visualization during surgical resection of malignant glioma.

Optical-assisted surgery is gaining ground in the clinical arena with several clinical trials underway to evaluate the performance of fluorescence-guided resection in several cancer types. The advantage of fluorescence-guided surgery is that it localizes diseased tissue that would otherwise remain undetected under white light. In phase III clinical trials, oral administration of 5-aminolevulinic acid (5-ALA), which is converted in metabolically active cells to a fluorescent compound (protoporphyrin IX), preferentially accumulates in tumour cells and can be measured in the red range. Clinical application using 5-ALA for fluorescent-guided surgical resection of GBM has shown positive results with 54-70% of cases achieving total resection[10,11] and an improved 9.5 month progression free survival.[12,13] While these results are promising, there may be significant room for improved tumour imaging given that there is potential for greater tissue attenuation when imaging with the 5-ALA derivative, protoporphyrin IX because it absorbs blue light (approximately 400 nm) and emits in the red range (approximately 640 nm). In this bandwidth, there is significantly less tissue penetration and higher autofluorescence compared to working in the near-infrared (NIR) range (~800 nm). Despite these limitations, 5-ALA in malignant glioma surgery was one of the

first 'proof-of-principle' agents to confirm that fluorescent-guided surgery could be used to improve surgical resections.

With the frequent overexpression of epidermal growth factor receptor (EGFR) in GBM and the safety and specificity of FDA-approved monoclonal antibodies (mAbs), antibody targeting of aberrantly expressed EGFR offers great potential to provide robust tumour localization in GBM.[14, 15] The feasibility of mAb use for targeting glioma is based on the several clinical trials currently ongoing to evaluate mAb therapy in glioma (clinicaltrials.gov identifier: NCT01475006, NCT01884740, NCT01238237). EGFR is overexpressed or mutated in 40% of GBM, and is expressed at very low levels in normal brain.[16] Recent studies have demonstrated sensitive and specific cancer imaging for fluorescent-guided resection using NIR probes conjugated to FDA approved mAb in several cancer types.[17-25] Recently, the technique was translated into patients with a phase I dose-escalation trial to determine the safety profile of cetuximab-IRDye 800CW in subjects with head and neck cancer (PI: E. Rosenthal, clinicaltrials.gov identifier: NCT01987375).

The objective of the current study was to determine if cetuximab-IRDye800CW (henceforth referred to as cetuximab-IRDye800) can be used to detect and assist cancer resection in animal models of GBM. A wide-field, intraoperative NIR imaging device (Luna, Novadaq, Bonita Springs, FL), which is currently FDA-approved for imaging vascular perfusion, was used to localize IRDye800 fluorescence in situ. In addition, a closed-field NIR imaging device (Pearl, LI-COR Biosciences, Lincoln, NE) and fluorescence scanner (Odyssey, LI-COR) was used to validate accumulation of cetuximab-IRDye800 in tumour and normal tissue via fluorescence localization. Fluorescence-guided surgical resection of cancer using FDA-approved agents and instrumentation accelerates the translation of this approach.

METHODS

CELL LINES AND ANIMAL MODELS

Cell lines and animal models were maintained and generated by the UAB Brain Tumour Animal Models Core Facility (USPHS NIH P20 CA151129). Human glioma cell lines D-54MG and U-251MG were gifts from Darell D. Bigner (Duke University, Durham NC), and U-87MG was procured from the American Tissue Type Collection (Manassas, VA) and maintained in Dulbecco's Modified Eagle's Medium (DMEM)/F12 with 7% fetal bovine serum and 2.6mM L-glutamine. Cells were cultured at 37°C and 5% CO_2, passaged at 70-90% confluence, and harvested with 0.05% trypsin/0.53mM EDTA. For the animal models, athymic female nude mice (aged 6-8 weeks) were obtained from Frederick Cancer Research (Frederick, MD). Cell

lines were genetically modified with a luciferase-expressing construct (Addgene, Cambridge, MA). For subcutaneous inoculation, $2x10^6$ D-54MG, U-251MG, or U-87MG cells (n=5) were implanted in the right midsection. Three weeks post implant (average tumour size: $188.3\pm15mm^3$), mice were stratified into equal groups based on tumour luciferase expression by bioluminescence imaging (BLI, IVIS-100, Caliper Life Sciences, Waltham, MA). For intracranial inoculation, approximately $5x10^5$ D-54MG or U-251MG cells (n=5) in 5µl of methylcellulose were injected 2mm anterior and 1mm lateral to the bregma at a depth of 2mm over 2min for adequate perfusion. Tumour formation and growth was monitored every three days via BLI. Approximately 2 weeks post implant, mice were stratified into equal groups based on tumour BLI. Institutional Animal Care and Use Committee (IACUC) at the University of Alabama at Birmingham approved all animal protocols (APN 130908793; 140310064).

CETUXIMAB-IRDYE800 CONJUGATION

Conjugation of cetuximab to IRDye800 was performed under cGMP conditions as previously reported (Zinn et al, Mol Imaging Biol, In Press). Briefly, cetuximab® (ImClone LLC, subsidiary of Eli Lilly and Company, Branchburg, NJ) was concentrated and pH adjusted by buffer exchange to a 10mg/ml solution in 50mM potassium phosphate, pH 8.5. IRDye800CW NHS ester (LI-COR) was conjugated to cetuximab for 2hrs at 20°C in the dark, at a molar ratio of 2.3:1. After column filtration to remove unconjugated dye and exchange buffer to phosphate buffered saline (PBS), pH 7, the final protein concentration adjusted to 2mg/ml, the product was sterilized by filtration and placed into single use vials and stored at 4°C until used.

Image acquisition and analysis: All groups received 0.1mg cetuximab-IRDye800 ($25mg/m^2$, 1/10 therapeutic cetuximab dose) intravenously (tail vein) prior to daily imaging with the NIR wide-field Luna system (Novadaq) and NIR closed-field Pearl system (LI-COR). Imaging was performed for 11 days post agent injection. During injections and imaging procedures, mice were anesthetized using vaporized isoflurane. For closed-field image analysis, mean fluorescent intensity (MFI), defined as total counts/region of interest (ROI) pixel area, was calculated using custom ROI generated for each specimen using integrated instrument software (ImageStudio, LI-COR). Tumour-to-background ratio (TBR) was calculated using MFI from tumour divided by MFI of peritumoural tissue. For BLI acquisitions, animals were injected intraperitoneally (IP) with 2.5mg D-luciferin (122796, Perkin Elmer, Waltham, MA) followed by a 15min perfusion period. All animals were then imaged for bioluminescence expression using the IVIS-100 system. Instrument acquisition settings were kept constant throughout study. For quantification of BLI signal, integrated instrument software was used to create size-matched ROIs, which were placed over tumour and total counts recorded.

SURGICAL PROCEDURES

All surgical procedures were performed by a UAB surgical resident (M. Korb). Twelve days post (subcutaneous model) or three days post (orthotopic model) cetuximab-IRDye800 injection; animals received 2.5mg D-luciferin IP 15min prior to sacrificing for tumour resection. After euthanasia by cervical dislocation, the skin (covering the tumour) and/or skullcap was removed and exposed tumour mass or brain was imaged (pre-resection acquisition) with closed-field and wide-field systems. After pre-resection imaging, tumours were excised using white light followed by BLI imaging of the wound bed. Using wide-field imaging, residual fluorescence tumour was removed and BLI imaging was again performed to confirm the presence of luciferase-positive cancer cells. For final BLI measurement, a luciferin reagent with ATP-Mg^{2+} (Promega, E1483, Madison, WI) was bathed and incubated on the wound bed for 10min prior to imaging.

IMMUNOHISTOCHEMISTRY

Fluorescence immunohistochemistry was performed as previously described.[20] Five μm sections were cut from the paraffin blocks and antigen retrieval was accomplished by heating in 1mM EDTA, pH 9.0, for 10min at 90°C. Samples were cooled to room temperature and blocked with 5% BSA in TBST for 5min at room temperature. A rabbit anti-EGFR antibody (ab2430, abcam, Cambridge, MA) was used to characterize EGFR expression and a mouse anti-factor VIII (ab139391, abcam, Cambridge, MA) was used to characterize vessel density via factor VIII. Primary antibodies were applied at the recommended concentrations and incubated overnight at 4°C. After washing, an anti-rabbit IgG-Alexa 546 antibody (A-11035, Life Technologies, Carlsbad, CA) was applied followed by an anti-mouse IgG-Alexa 488 antibody (A-11001, Life Technologies, Carlsbad, CA) at manufacturer recommendation. After washing, slides were imaged by a blinded operator (J. Kovar) using an Olympus IX81 Inverted Microscope equipped with a halogen bulb and following filters (Alexa 488: EX 488/20, DC495LP; EM 525/50; Alexa 546: EXET545/30x, T570LP, EM ET620/60M; IRDye800: EX: HQ760/40x, 790DCXR, EM: HQ830/50m; Chroma Technology Corp., Rockingham, VT).

STATISTICAL ANALYSIS

All statistical analyses were performed using SPSS 21.0 (SPSS Inc, Chicago, IL, USA). Descriptive statistics were calculated for variables of interest. A Student's t test was used to determine the statistical significance unless otherwise stated. Linear regression was used to assess associations between described metrics (i.e. EGFR/factorVIII or bioluminescence/fluorescence). P-values <0.05 were considered statistically significant. Data with error bars represent mean ± SD.

RESULTS

CETUXIMAB-IRDYE800 IN A SUBCUTANEOUS XENOGRAFT MODEL OF MALIGNANT GLIOMA

To evaluate the potential of Cetuximab-IRDye800 to provide sufficient fluorescence contrast to differentiate between disease and surrounding normal tissue, a subcutaneous model was used due to the improved tolerance of the animals, permitting longer study duration for optimal characterization of fluorescence changes over time. As shown in Figure 1a, D-54MG xenograft tumours exhibited a 2.7-fold increase in fluorescence, or TBR, compared to surrounding normal tissue at 24hrs post cetuximab-IRDye800 injection, when imaged using the closed-field Pearl system. The same results were also seen for the U-251MG (Fig. 1b) and

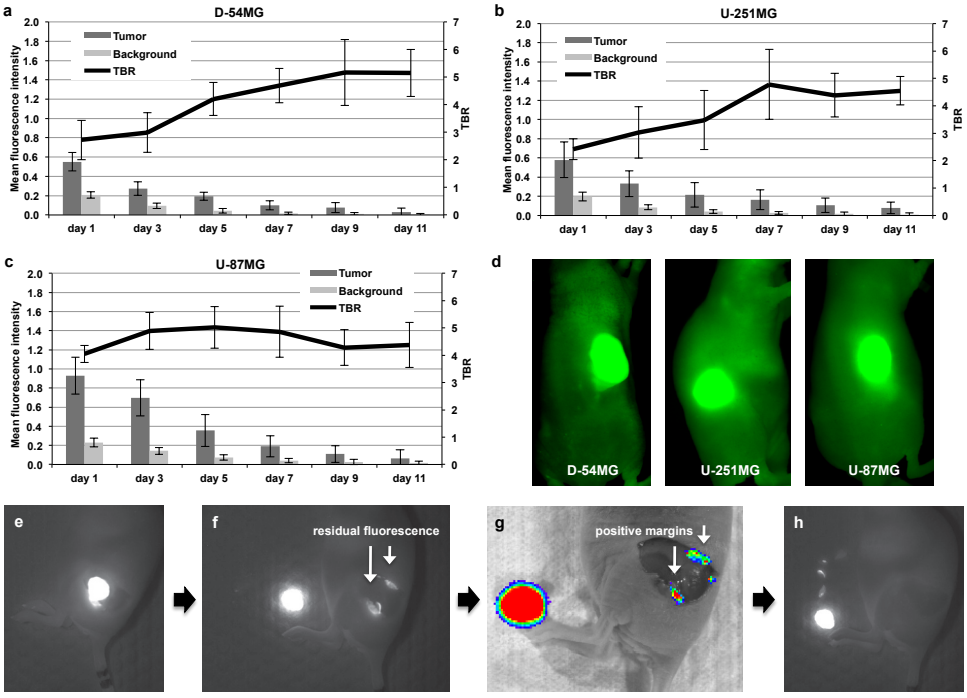

Figure 1 Cetuximab-IRDye 800CW in a subcutaneous xenograft model of malignant glioma. *Cetuximab-IRDye 800CW was systemically injected (tail vein) in athymic nude mice bearing (a) D-54MG tumours, (b) U-251MG tumours, and (c) U-87MG tumours. Mice were imaged using closed-field system over 11 days. Tumour mean pixel intensity, background mean pixel intensity, and tumour-to-background ratio (TBR) were recorded. (d) Fluorescent images using the closed-field system are shown of respective tumours receiving cetuximab-IRDye 800CW on day 3 post administration. (e-h) Fluorescent images of representative luciferase positive D-54MG tumour resection shows (e) skin removed, (f) tumour resection revealing positive fluorescence margins, (g) residual tumour confirmed using bioluminescence imaging, and (h) complete resection of positive margins as determined by fluorescent imaging. Values are mean fluorescence intensity and TBR ± SD.*

U-87MG (Fig. 1c) cell lines, with a TBR of 2.5 and 4.0, respectively, at 24hrs post injection. This trend continued at each imaging time point with a significantly ($P<0.05$) greater MFI in the tumour compared to normal surrounding tissue. Additionally, the TBR was also shown to increase over time for the D-54MG and U-251MG tumours with a significantly ($P<0.05$) greater TBR at day 11 versus day 1 post cetuximab-IRDye800 injection. For the U-87MG cell tumour, there was no significant difference in TBR over time. However, the average TBR between the cell lines was not significantly ($P=0.35$) different at day 11. When the TBR values were averaged across the study duration, U-87MG had the highest (4.5) followed by D-54MG (4.1) and U-251MG (3.7). Representative images are shown in Figure 1d of mice bearing D-54MG, U-251MG, and U-87MG tumours acquired using the closed-field fluorescence instrument on day 3 post cetuximab-IRDye800 injection.

On day 11, tumours were surgically resected from the mouse flank using white light. As shown in Figure 1e, once the skin was removed from each tumour, fluorescence imaging was performed using the wide-field instrument. Figure 1f shows wide-field fluorescence imaging of post-resection wound bed revealing presence of residual fluorescence, which was confirmed

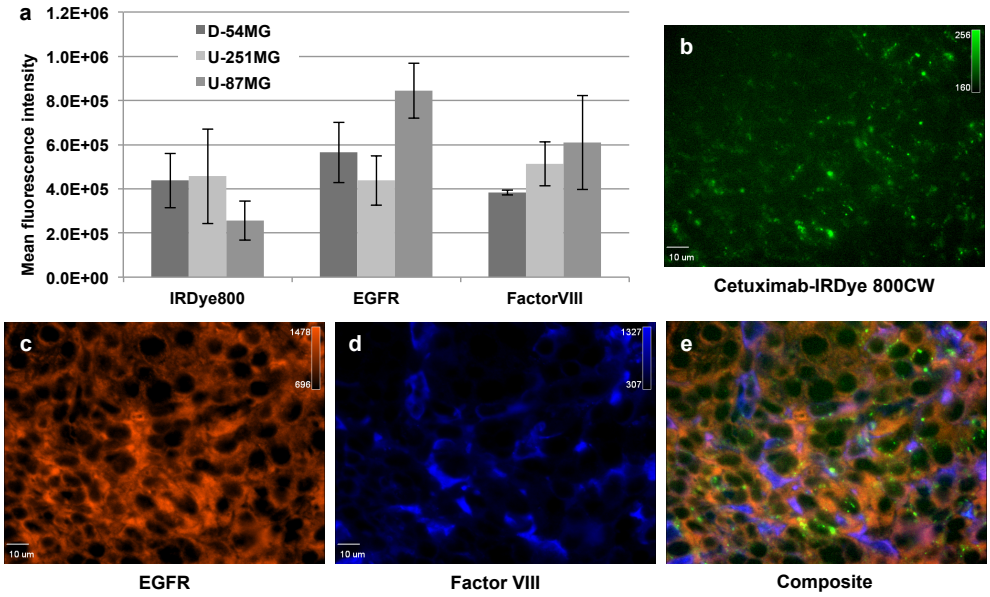

Figure 2 Fluorescence immunohistochemistry and cell staining of malignant glioma. *(a) Quantification of histological sections of resected D54, U251, and U87 flank tumors fluorescently probed for EGFR and factorVIII. Values are mean fluorescence counts +/- standard deviation. Representative 40x microscopic images are shown of fluorescence immunohistological staining for (b) cetuximab-IRDye800 accumulation, (c) EGFR expression, (d) factor VIII expression, and (e) corresponding composite from a U251 tumor.*

to be tumour using bioluminescence imaging (Fig. 1g). In Figure 1h, wide-field fluorescence imaging was used to remove residual tumour tissue.

COMPARISON OF EGFR EXPRESSION, VESSEL DENSITY, AND FLUORESCENCE AMONG CELL LINES

To evaluate cellular and intratumoural characteristics affecting cetuximab-IRDye800 tumour accumulation, as determined using fluorescence imaging, relative EGFR expression and vessel density were measured. As shown in Figure 2a, U-87MG tumours ($8.4x10^5 \pm 1.2x10^4$ MFI) had significantly (P=0.009) greater EGFR expression over D-54MG tumours ($5.6x10^5 \pm 1.3x10^4$ MFI) when EGFR expression was measured in resected tumours using immunohistochemistry. Likewise, D-54MG EGFR expression was significantly (P=0.04) greater than U-251MG EGFR expression ($4.3x10^5 \pm 1.1x10^4$ MFI). When vessel density was evaluated, U-87MG had the highest expression of factor VIII relative to U-251MG (P=0.22) and D-54MG (P=0.001). When IRDye800 fluorescence was measured in slide-mounted tumour sections, D-54MG ($4.3x10^5 \pm 1.2x10^5$ MFI) and U-251MG ($4.3x10^5 \pm 1.2x10^5$ MFI) were not significantly (P=0.78) different while U-87MG ($2.5x10^5 \pm 8.8x10^4$ MFI) was significantly (P=0.04) lower than D-54MG. Univariate analysis showed a strong association between the EGFR expression and fluorescence intensity in D-54MG and U-251MG tumours (P<0.001 and P=0.02, respectively). No association between the EGFR expression and fluorescence intensity in U-87MG tumours were seen (P > 0.05). U-87MG vascular density, however, showed a strong association with the fluorescence intensity (P<0.001), while D-54MG and U-251MG did not (P>0.05). Representative fluorescence microscopy (40x) images from a U-251MG tumour reveal cetuximab-IRDye800 accumulation (Fig. 2b), EGFR expression (Fig. 2c), and factor VIII expression (Fig. 2d). Figure 2e shows composite image of each fluorescent channel.

FLUORESCENCE-GUIDED TUMOUR RESECTION IN AN ORTHOTOPIC MODEL OF MALIGNANT GLIOMA USING D-54MG CELLS

To evaluate the fluorescence contrast of systemically administered cetuximab-IRDye800 for disease delineation in a surgical setting with human glioma; an orthotopic animal model was generated using luciferase positive D-54MG or U-251MG cells. In Figure 3a, representative images are shown of BLI, wide-field fluorescence imaging, and closed-field fluorescence imaging of skin and skullcap removed in a mouse bearing D-54MG orthotopic tumour. The tumour, which is localized using BLI, is shown to be brightly fluorescent during imaging acquisition using the respective instruments. A pre-resection (skin and skullcap removed) TBR of 8.6 ± 3.4 was calculated for the closed-field system while a TBR of 23.2 ± 5.1 was calculated for the wide-field, intraoperative system. Figure 3b shows BLI, wide-field, and closed-

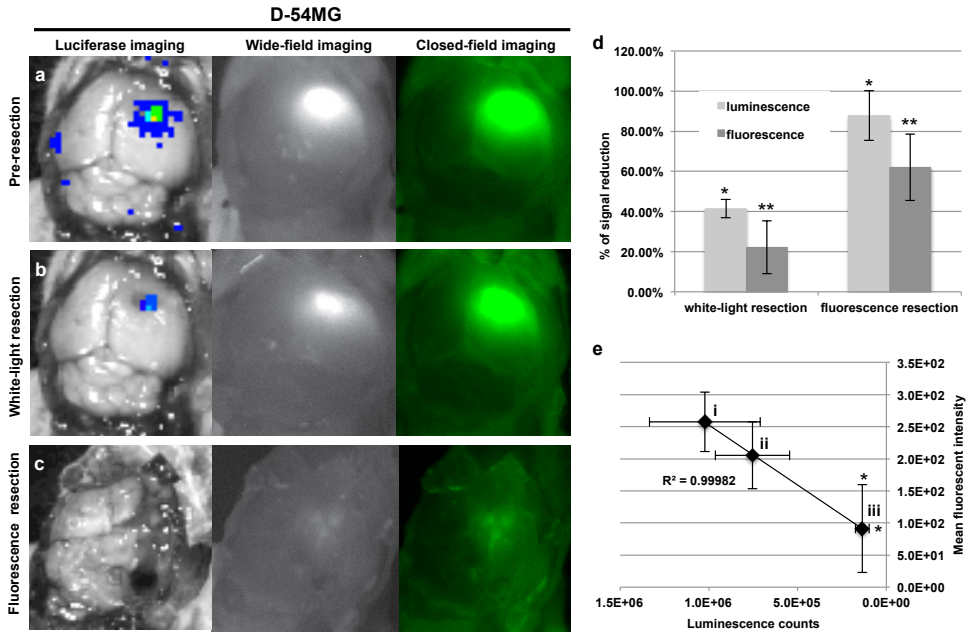

Figure 3 Qualitative analysis of cetuximab-IRdye800 in an orthotopic xenograft model of malignant glioma using D54 cells. *Cetuximab-IRDye800 was systemically injected (tail vein) in athymic nude mice bearing orthotopic bioluminescent positive D54 tumors. Fluorescence (Luna and Pearl imaging systems) and bioluminescent images were acquired during (a) pre-resection (skin and skullcap removed), (b) post-optical resection, and (c) post-fluorescence resection at day 3 post cetuximab-IRDye800 injection. (d) Percent of signal reduction from pre-resection was calculated using fluorescent and bioluminescent imaging at post-optical imaging and post-fluorescent imaging time points. (e) Regression analysis was performed by plotting fluorescence signal (y-axis) against luminescence signal (x-axis) at (i) pre-resection, (ii) post-optical resection, and (iii) post-fluorescent resection. Error bars are standard deviation and asterisks denote p<0.05.*

field imaging acquired post conventional white-light resection of the orthotopic tumour. BLI, wide-field, and closed-field imaging post fluorescence-guided resection is shown in Figure 3c. Quantification of BLI and fluorescence (Fig. 3d) revealed a 41% reduction in bioluminescence signal and 22% reduction in fluorescence signal, relative to pre-resection values, was achieved using white-light resection. However, there was a significantly greater reduction in luminescence (87%, P=0.001) and fluorescence (62%, P=0.004) observed when using fluorescence-guided resection. In Figure 3e, regression analysis revealed a significant correlation (R^2=0.99) between fluorescence and luminescence signal at (i) pre-resection, (ii) post-optical resection, and (iii) post-fluorescent resection. Importantly, a significant decrease in luminescence (P=0.02) and fluorescence (P=0.04) signal was observed after fluorescence resection, but not white-light resection (P>0.05).

FLUORESCENCE-GUIDED TUMOUR RESECTION IN AN ORTHOTOPIC MODEL OF MALIGNANT GLIOMA USING U-251MG CELLS

Using a cell line of contrasting EGFR expression relative to D-54MG, similar results were observed for the U-251MG tumours. In Figure 4a, representative images are shown of BLI, wide-field fluorescence imaging, and closed-field fluorescence imaging of a mouse bearing U-251MG orthotopic tumour with skin and skullcap removed. The tumour, which is localized using BLI, is shown to be brightly fluorescent during imaging acquisition using the respective instruments. A pre-resection (skin and skullcap removed) TBR of 7.2 ± 2.6 was calculated for the closed-field system while a TBR of 19.5 ± 4.2 was calculated for the wide-field, intraoperative system. Figure 4b shows BLI, wide-field, and closed-field imaging acquired post conventional white-light resection of the orthotopic tumour. BLI, wide-field, and closed-field imaging post fluorescence-guided resection is shown in Figure 4c. For the U-251MG tumour, white-light resection achieved a 70% reduction in bioluminescence signal and 20%

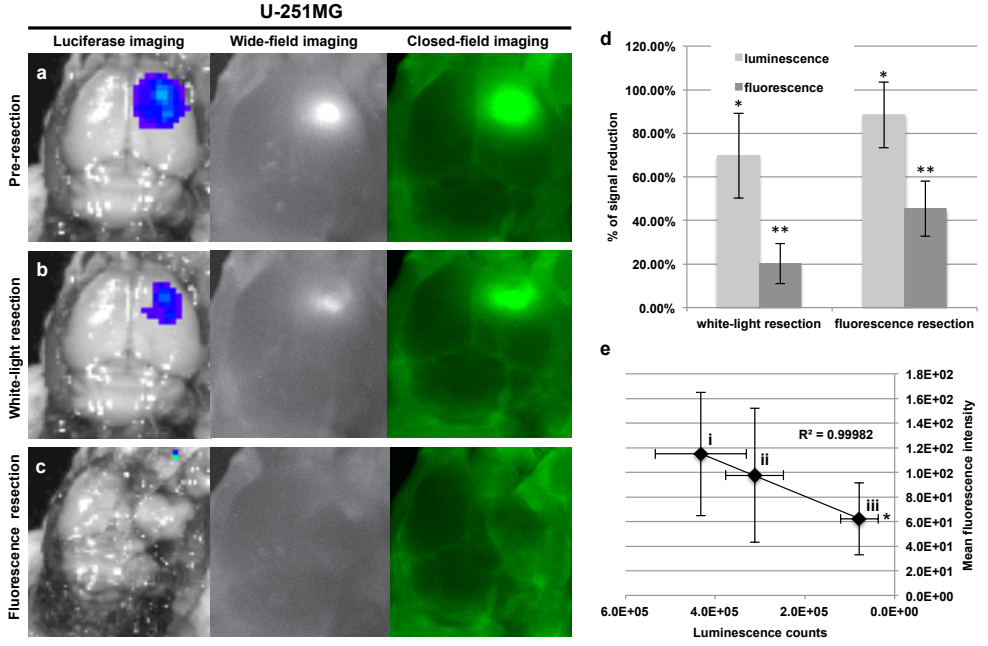

Figure 4 Qualitative analysis of cetuximab-IRdye800 in an orthotopic xenograft model of malignant glioma using U251 cells. *Cetuximab-IRDye800 was systemically injected (tail vein) in athymic nude mice bearing orthotopic bioluminescent positive U251 tumors. Fluorescence (Luna and Pearl imaging systems) and bioluminescent images were acquired during (a) pre-resection (skin and skull-cap removed), (b) post-white-light resection, and (c) post-fluorescence resection at day 3 post cetuximab-IRDye800 injection. (d) Percent of signal reduction from pre-resection was calculated using fluorescent and bioluminescent imaging at post-optical imaging and post-fluorescent imaging time points. (e) Regression analysis was performed by plotting fluorescence signal (y-axis) against luminescence signal (x-axis) at (i) pre-resection, (ii) post-optical resection, and (iii) post-fluorescent resection. Error bars are standard deviation and asterisks denote P<0.05.*

reduction in fluorescence signal, relative to pre-resection values (Figure 4d). Just as with the previous cell line, there was a significantly greater reduction in luminescence (88%, P=0.008) and fluorescence (45%, P=0.007) observed for U-251MG tumour resection when using fluorescence-guidance. Regression analysis revealed a significant correlation (R2=0.99) between fluorescence and luminescence signal at (i) pre-resection, (ii) post-optical resection, and (iii) post-fluorescent resection (Figure 4e). For the U-251MG tumours, there was a significant decrease in luminescence (P=0.03) and fluorescence (P=0.02) signal that was observed after fluorescence resection.

DISCUSSION

The objective of this study was to evaluate the capacity of systemically administered cetuximab-IRDye800 to provide sufficient contrast for fluorescence-guided resection of GBM. The optical probe consists of a commercially available NIR dye conjugated to an FDA-approved mAb to specifically target and optically localize cancer. We have previously shown that the covalent conjugation of these molecules does not alter the dye properties or binding affinity of the antibody and the conjugate remains intact post systemic administration.[26] When evaluating the fluorescence-guided resection strategy in an orthotopic model, luciferase positive cells were used to permit real-time localization of residual tumour during post-mortem resections of GBM in situ. Utilizing this dual-modality approach, we demonstrated that a significantly greater amount of tumour was removed using fluorescence-guided resection compared to white-light resection in both the D-54MG and U-251MG tumours, as determined by bioluminescence signal reduction. When results from fluorescence and bioluminescence imaging were compared at each imaging time point, there was a significant correlation between the two signals, demonstrating that the fluorescence generated from the cetuximab-conjugated IRDye800 molecule was associated with the luciferase positive tumour tissue. The results from the orthotopic models also confirmed the ability of the antibody-dye conjugate to extravasate and invade the diseased tissue due to the breakdown of the blood brain barrier commonly associated with glioma.[27] While it was not practicable to perform survival surgery on the orthotopic mouse model for this proof-of-principle study, the size of these tumours represents an excellent example of residual tumour following a more extensive resection that would likely be performed in patients. As such, the ability to identify intraoperatively what would represent residual tumour in patients readily suggests the obvious potential of this adjunct.

During the study, multiple GBM cell lines were used in both subcutaneous and orthotopic animal models. The subcutaneous model was used due to the improved tolerance of the animals for this tumour location, permitting longer study duration to identify the optimal day to perform surgery. Results of the subcutaneous modeling showed that TBR increased over time for the D-54MG and U-251MG tumours with a significantly greater TBR at day 11 versus day 1 post cetuximab-IRDye800 injection. Considering the tumour fluorescence did not increase over time, the observed increase in TBR was due to a slower rate of fluorescence clearance within the tumour compared to surrounding normal tissue. In the U-87MG tumour, the rate of fluorescence clearance was similar between the tumour and background tissue leading to no significant difference in TBR over time. This was due to the higher tumour fluorescence observed in the U-87MG tumours at earlier time points relative to the D-54MG and U-251MG tumours. Univariate analysis showed a strong association between EGFR expression and fluorescence intensity for D-54MG and U-251MG tumours while no association between the EGFR expression and fluorescence intensity was seen for U-87MG tumours. U-87MG vascular density, however, showed a strong association with the fluorescence intensity, while D-54MG and U-251MG did not. These results suggest that the increase in vessel density within the U-87MG tumours led to relatively higher fluorescence due to a higher blood-pool volume found within these tumours. The greater vessel density observed in the U-87MG tumours is consistent with similar studies evaluating vascularity and anti-angiogenic treatments.[28-30] However, the average TBR between the cell lines was not significantly (P=0.35) different at day 11. When the TBR was calculated during daily imaging, albeit attenuated by skin, values were averaged across the study duration revealing U-87MG to have highest (4.5) followed by D-54MG (4.1) and U-251MG (3.7).

With new fluorescence-guided resection strategies quickly being introduced, the success of the strategy does not solely depend on the achieved signal intensity targeted within the tissue of interest. Successful approaches must achieve greater accumulation of the respective probe in the tumour relative to normal surrounding tissue. The TBR (3-5) produced during the study was sufficient to assist in tumour localization in subcutaneous models. In the orthotopic models, the TBR was calculated to range from 19-23 for the intraoperative instrument (Luna) on the day of surgery. TBRs in this range have been proven successful for disease localization in situ when using NIR imaging strategy.[17-20,26,31] In a similar study evaluating an integrin-targeted peptide conjugated to IRDye800, investigators measured an average TBR of 2.5 during intravital daily imaging of multiple GBM animal models.[32] Ex vivo imaging of tumour-bearing brains showed an average TBR of 42 between the multiple cell lines tested. While the generation of this ratio of tumour to normal tissue fluorescence is subject to background

value origin, similar studies evaluating antibody-based approaches to fluorescence-guided resection in other cancer types have shown similar TBR values sufficient for successful delineation and surgical resection of disease.[19,22,31,33]

In the orthotopic fluorescence images produced during the study, low-level fluorescence intensity is shown in normal areas of the brain surrounding the tumor. This may be perceived as non-specific fluorescence due to antibody accumulation in uninvolved areas of the brain. However, as with most photon based imaging techniques, the perception of specificity can be adjusted using thresholding of the color map using onboard instrument software. By adjusting the thresholding, the upper and lower limits of photon intensity per pixel can be gated for the entire image. The threshold values (upper and lower limits on the color look up table) were maintained constant for all images shown. In order to keep these values consistent between cell lines, the lower limit value had to be low enough to demonstrate fluorescence signal in the weakest cell line. When this value was applied to the higher fluorescing cell line, the scattering of fluorescence intensity is shown in the surrounding normal tissue. If the thresholding was tailored for each cell line, the lower intensity pixels would not be assigned color and the signal would appear specific to the tumor. The authors chose keep the thresholding constant throughout the study in order to show the differences in fluorescence intensity between cell lines.

This approach to fluorescence-guided resection of GBM is a viable candidate for entry into the clinical arena for multiple reasons. Firstly, the monoclonal antibody is FDA-approved and targets a receptor with the greatest overexpression in GBM.[14, 15] In addition, clinical trials evaluating cetuximab in GBM have been performed[34] and are ongoing (clinicaltrials.gov identifier: NCT01884740, NCT01238237). Secondly, the toxicity of IRDye800 has been evaluated in a preclinical model and the FDA currently holds a drug master file for the NIR molecule.[35] In addition, current neurosurgery microscopes (Zeiss and Leica brands) are designed to image NIR dyes and are already in place in most operating rooms. Lastly, the toxicity of cetuximab-IRDye800 has been assessed in non-human primates (Zinn et al, Mol Imaging Biol, In Press) and is currently being evaluated in a phase 1, open label study assessing the safety and pharmacokinetics of escalating doses (clinicaltrials.gov identifier: NCT01987375). A secondary objective of this phase 1 study is to evaluate cetuximab-IRDye800 as an optical imaging agent to detect head and neck squamous cell carcinoma during surgical procedures.
The use of cetuximab-IRDy800 to target glioma for fluorescence-guided surgery is viable strategy considering EGFR has the unique classification of being the most aberrantly expressed gene in glioma, making it a robust target for fluorescence-guided surgery.[14, 15] By tar-

geting EGFR for imaging, therapeutic barriers, such as KRAS mutation, are not a limitation considering constitutive tyrosine kinase signaling does not affect the ability of a mAb to target and bind EGFR. Additionally, It has been shown that expression levels of EGFR (both wild type and mutant) directly correlate with the grade of the tumour. For example, studies have revealed that 60% of primary GBMs display an overexpression of EGFR compared to 10% prevalence for secondary GBM.[36, 37] Also, more than 90% of GBMs are primary GBMs, meaning they developed without evidence of an earlier lower-grade astrocytoma.[37]

CONCLUSION

Here, cetuximab-IRDye800 was shown to provide sufficient contrast for disease localization in mouse models of GBM. This study represents the first full antibody-based approach to fluorescence-guided surgical resection of GBM in preclinical models. Implementation of this strategy would introduce the first immuno-based approach to fluorescence-guided surgery in GBM resection, utilizing the most aberrantly expressed molecular marker and a superior fluorescence probe leading to higher signal contrast than what is currently available.
The authors have no conflict of interest

ACKNOWLEDGMENTS

Support for the study was provided by the UAB Brain Tumour Core Facility (USPHS NCI P20CA151129), UAB Comprehensive Cancer Center small animal core facility (P30 CA013148), and NIH grants 5T32CA091078-12, R21CA179171.

REFERENCES

1. Chaichana KL, Jusue-Torres I, Navarro-Ramirez R, Raza SM, Pascual-Gallego M, Ibrahim A, Hernandez-Hermann M, Gomez L, Ye X, Weingart JD, Olivi A, Blakeley J, Gallia GL, Lim M, Brem H, Quinones-Hinojosa A. Establishing percent resection and residual volume thresholds affecting survival and recurrence for patients with newly diagnosed intracranial glioblastoma. Neuro Oncol. 2014 Jan;16(1):113-22.
2. Lacroix M, Abi-Said D, Fourney DR, Gokaslan ZL, Shi W, DeMonte F, Lang FF, McCutcheon IE, Hassenbusch SJ, Holland E, Hess K, Michael C, Miller D, Sawaya R. A multivariate analysis of 416 patients with glioblastoma multiforme: prognosis, extent of resection, and survival. J Neurosurg. 2001 Aug;95(2):190-8.
3. Sanai N, Polley MY, McDermott MW, Parsa AT, Berger MS. An extent of resection threshold for newly diagnosed glioblastomas. J Neurosurg. 2011 Jul;115(1):3-8.
4. Bloch O, Han SJ, Cha S, Sun MZ, Aghi MK, McDermott MW, Berger MS, Parsa AT. Impact of extent of resection for recurrent glioblastoma on overall survival: clinical article. J Neurosurg. 2012 Dec;117(6):1032-8.
5. Giese A, Bjerkvig R, Berens ME, Westphal M. Cost of migration: invasion of malignant gliomas and implications for treatment. J Clin Oncol. 2003 Apr 15;21(8):1624-36.
6. Goebell E, Fiehler J, Ding XQ, Paustenbach S, Nietz S, Heese O, Kucinski T, Hagel C, Westphal M, Zeumer H. Disarrangement of fiber tracts and decline of neuronal density correlate in glioma patients--a combined diffusion tensor imaging and 1H-MR spectroscopy study. AJNR Am J Neuroradiol. 2006 Aug;27(7):1426-31.
7. Engelhorn T, Savaskan NE, Schwarz MA, Kreutzer J, Meyer EP, Hahnen E, Ganslandt O, Dörfler A, Nimsky C, Buchfelder M, Eyüpoglu IY. Cellular characterization of the peritumoral edema zone in malignant brain tumors. Cancer Sci. 2009 Oct;100(10):1856-62.
8. Keles GE, Lamborn KR, Berger MS. Low-grade hemispheric gliomas in adults: a critical review of extent of resection as a factor influencing outcome. J Neurosurg. 2001 Nov;95(5):735-45.
9. Johannesen TB, Langmark F, Lote K. Progress in long-term survival in adult patients with supratentorial low-grade gliomas: a population-based study of 993 patients in whom tumors were diagnosed between 1970 and 1993. J Neurosurg. 2003 Nov;99(5):854-62.
10. Cortnum S, Laursen R. [Fluorescence-guided surgery with 5-aminolevulinic acid for resection of malignant gliomas--a new treatment modality].

Ugeskr Laeger. 2013 Feb 25;175(9):570-3.

11. Tykocki T, Michalik R, Bonicki W, Nauman P. Fluorescence-guided resection of primary and recurrent malignant gliomas with 5-aminolevulinic acid. Preliminary results. Neurol Neurochir Pol. 2012 Jan-Feb;46(1):47-51.
12. 1Stummer W, Pichlmeier U, Meinel T, Wiestler OD, Zanella F, Reulen HJ; ALA-Glioma Study Group. Fluorescence-guided surgery with 5-aminolevulinic acid for resection of malignant glioma: a randomised controlled multicentre phase III trial. Lancet Oncol. 2006 May;7(5):392-401.
13. Aldave G, Tejada S, Pay E, Marigil M, Bejarano B, Idoate MA, Díez-Valle R. Prognostic value of residual fluorescent tissue in glioblastoma patients after gross total resection in 5-aminolevulinic Acid-guided surgery. Neurosurgery. 2013 Jun;72(6):915-20; discussion 920-1.
14. Heimberger AB, Hlatky R, Suki D, Yang D, Weinberg J, Gilbert M, Sawaya R, Aldape K. Prognostic effect of epidermal growth factor receptor and EGFRvIII in glioblastoma multiforme patients. Clin Cancer Res. 2005 Feb 15;11(4):1462-6. 15;11(4):1462-6.
15. Bredel M, Pollack IF, Hamilton RL, James CD. Epidermal growth factor receptor expression and gene amplification in high-grade non-brainstem gliomas of childhood. Clin Cancer Res. 1999 Jul;5(7):1786-92.16.
16. Gan HK, Kaye AH, Luwor RB. The EGFRvIII variant in glioblastoma multiforme. J Clin Neurosci. 2009 Jun;16(6):748-54.
17. 1Day KE, Beck LN, Deep NL, Kovar J, Zinn KR, Rosenthal EL. Fluorescently labeled therapeutic antibodies for detection of microscopic melanoma. Laryngoscope. 2013 Nov;123(11):2681-9.
18. Day KE, Beck LN, Heath CH, Huang CC, Zinn KR, Rosenthal EL. Identification of the optimal therapeutic antibody for fluorescent imaging of cutaneous squamous cell carcinoma. Cancer Biol Ther. 2013 Mar;14(3):271-7.
19. Day KE, Sweeny L, Kulbersh B, Zinn KR, Rosenthal EL. Preclinical comparison of near-infrared-labeled cetuximab and panitumumab for optical imaging of head and neck squamous cell carcinoma. Mol Imaging Biol. 2013 Dec;15(6):722-9.
20. Heath CH, Deep NL, Sweeny L, Zinn KR, Rosenthal EL. Use of panitumumab-IRDye800 to image microscopic head and neck cancer in an orthotopic surgical model. Ann Surg Oncol. 2012 Nov;19(12):3879-87.
21. Kim GP, Grothey A. Targeting colorectal cancer with human anti-EGFR monoclonocal antibodies: focus on panitumumab. Biologics. 2008 Jun;2(2):223-8.
22. Kulbersh BD, Duncan RD, Magnuson JS, Skipper JB, Zinn K, Rosenthal EL. Sensitivity and specificity of fluorescent immunoguided neoplasm detection in head and neck cancer xenografts. Arch

Otolaryngol Head Neck Surg. 2007 May;133(5):511-5.
23. Newman JR, Gleysteen JP, Barañano CF, Bremser JR, Zhang W, Zinn KR, Rosenthal EL. Stereomicroscopic fluorescence imaging of head and neck cancer xenografts targeting CD147. Cancer Biol Ther. 2008 Jul;7(7):1063-70.
24. Rosenthal EL, Kulbersh BD, Duncan RD, Zhang W, Magnuson JS, Carroll WR, Zinn K. In vivo detection of head and neck cancer orthotopic xenografts by immunofluorescence. Laryngoscope. 2006 Sep;116(9):1636-41.
25. Rosenthal EL, Kulbersh BD, King T, Chaudhuri TR, Zinn KR. Use of fluorescent labeled anti-epidermal growth factor receptor antibody to image head and neck squamous cell carcinoma xenografts. Mol Cancer Ther. 2007 Apr;6(4):1230-8.
26. Korb ML, Hartman YE, Kovar J, Zinn KR, Bland KI, Rosenthal EL. Use of monoclonal antibody-IRDye800CW bioconjugates in the resection of breast cancer. J Surg Res. 2014 May 1;188(1):119-28.27.
27. Tate MC, Aghi MK. Biology of angiogenesis and invasion in glioma. Neurotherapeutics. 2009 Jul;6(3):447-57.
28. Han M, Wang H, Zhang HT, Han Z. Expression of Tax-interacting protein 1 (TIP-1) facilitates angiogenesis and tumor formation of human glioblastoma cells in nude mice. Cancer Lett. 2013 Jan 1;328(1):55-64.
29. Lee CG, Heijn M, di Tomaso E, Griffon-Etienne G, Ancukiewicz M, Koike C, Park KR, Ferrara N, Jain RK, Suit HD, Boucher Y. Anti-Vascular endothelial growth factor treatment augments tumor radiation response under normoxic or hypoxic conditions. Cancer Res. 2000 Oct 1;60(19):5565-70.
30. Ricard C, Stanchi F, Rodriguez T, Amoureux MC, Rougon G, Debarbieux F. Dynamic quantitative intravital imaging of glioblastoma progression reveals a lack of correlation between tumor growth and blood vessel density. PLoS One. 2013 Sep 12;8(9):e72655.
31. Nguyen QT, Olson ES, Aguilera TA, Jiang T, Scadeng M, Ellies LG, Tsien RY. Surgery with molecular fluorescence imaging using activatable cell-penetrating peptides decreases residual cancer and improves survival. Proc Natl Acad Sci U S A. 2010 Mar 2;107(9):4317-22. 31.
32. Huang R, Vider J, Kovar JL, Olive DM, Mellinghoff IK, Mayer-Kuckuk P, Kircher MF, Blasberg RG. Integrin αvβ3-targeted IRDye 800CW near-infrared imaging of glioblastoma. Clin Cancer Res. 2012 Oct 15;18(20):5731-40.
33. Kaushal S, McElroy MK, Luiken GA, Talamini MA, Moossa AR, Hoffman RM, Bouvet M. Fluorophore-conjugated anti-CEA antibody for the intraoperative imaging of pancreatic and colorectal cancer. J Gastrointest Surg. 2008 Nov;12(11):1938-50.

34. Combs SE, Heeger S, Haselmann R, Edler L, Debus J, Schulz-Ertner D. Treatment of primary glioblastoma multiforme with cetuximab, radiotherapy and temozolomide (GERT)--phase I/II trial: study protocol. BMC Cancer. 2006 May 18;6:133.
35. Marshall MV, Draney D, Sevick-Muraca EM, Olive DM. Single-dose intravenous toxicity study of IRDye 800CW in Sprague-Dawley rats. Mol Imaging Biol. 2010 Dec;12(6):583-94.
36. Hatanpaa KJ, Burma S, Zhao D, Habib AA. Epidermal growth factor receptor in glioma: signal transduction, neuropathology, imaging, and radioresistance. Neoplasia. 2010 Sep;12(9):675-84.
37. Ohgaki H, Kleihues P. Genetic pathways to primary and secondary glioblastoma. Am J Pathol. 2007 May;170(5):1445-53.